Separation Science and Technology
Publication details, including instructions for authors and subscription information:
http://www.informaworld.com/smpp/title~content=t713708471

Modeling the Electrokinetic Decontamination of Concrete

Michael T. Harris[a]; David W. DePaoli[a]; Moonis R. Ally[a]
[a] Chemical Technology Division, Oak Ridge National Laboratory, Oak Ridge, Tennessee

To cite this Article Harris, Michael T. , DePaoli, David W. and Ally, Moonis R.(1997) 'Modeling the Electrokinetic Decontamination of Concrete', Separation Science and Technology, 32: 1, 827 — 848
To link to this Article: DOI: 10.1080/01496399708003232
URL: http://dx.doi.org/10.1080/01496399708003232

SEPARATION SCIENCE AND TECHNOLOGY, 32(1-4), pp. 827-848, 1997

MODELING THE ELECTROKINETIC DECONTAMINATION OF CONCRETE

Michael T. Harris, David W. DePaoli and Moonis R. Ally
Chemical Technology Division
Oak Ridge National Laboratory
Oak Ridge, Tennessee 37831-6224

ABSTRACT

The decontamination of concrete is a major concern in many Department of Energy (DOE) facilities. Numerous techniques (abrasive methods, manual methods, ultrasonics, concrete surface layer removal, chemical extraction methods, etc.) have been used to remove radioactive contamination from the surface of concrete. Recently, processes that are based on electrokinetic phenomena have been developed to decontaminate concrete. Electrokinetic decontamination has been shown to remove from 70 to over 90% of the surface radioactivity. To evaluate and improve the electrokinetic processes, a model has been developed to simulate the transport of ionic radionuclei constituents through the pores of concrete and into the anolyte and catholyte. The model takes into account the adsorption and desorption kinetics of the radionuclei from the pore walls, and ion transport by electro-osmosis, electromigration, and diffusion. A numerical technique, orthogonal collocation, is used to simultaneously solve the governing convective diffusion equations for a porous concrete slab and the current density equation.

This paper presents the theoretical framework of the model and the results from the computation of the dynamics of ion transport during electrokinetic treatment of concrete. The simulation results are in good agreement with experimental data.

INTRODUCTION

Approximately 1000 contaminated facilities have been identified in the DOE complex (1). Dickerson et al. (2) projected that approximately 86% of the contaminated

*Managed by Lockheed-Martin Energy Research Corporation, Inc. for the U.S. Department of Energy under contract
DE-AC05-84OR21400.

DOE process buildings have radiological contamination. The major radiological contaminants in the concrete of these buildings are ^{137}Cs, ^{238}U, ^{60}Co, and ^{90}Sr.

The nature of the contaminated concrete varies from loose and fixed surface contamination to that within joints and cracks. Surface contamination can be easily cleaned by mechanical surface removal technologies (e.g., scabbling/scarification, ultrahigh-pressure water and grit and shot blasting, etc.) and surface cleaning technologies (e.g. solvent washing, superheated water, steam cleaning, etc.) (2).

In reactor pools where the concrete is exposed to contamination under a hydrostatic head, extensive penetration of the contaminants into the concrete may occur (2). Under these circumstances, surface removal techniques are ineffective and techniques are needed to force the lixiviant deeper into the bulk of the concrete. One method for transporting the lixiviant deep into the pores of the bulk concrete involves applying a potential across the concrete mass. Electrical stresses at the liquid-vapor interface result in the penetration of the pores by the lixiviant (3). By soaking the concrete with the lixiviant, the contaminants are transferred from the solid phase to the aqueous phase as the lixiviant contacts and dissolves the contaminants that are sorbed on the walls and precipitated in the pores.

Electrokinetics can be used to remove charged contaminants (i.e., ions and charged particles) from liquid in the pores of concrete (4,5). The removal of charged contaminants by electrokinetics (EK) involves three mechanisms (i.e., electromigration, electroosmosis, and electrophoresis) that control the transport of contaminants through the pores in the concrete. Transport by molecular diffusion may also occur. Diffusive transport occurs due to concentration gradients in the pore. Electromigration involves the transport of charged ions in solution (6). Electroosmosis involves the movement of liquid containing ions relative to a stationary surface, such as a capillary pore (7,8). Electrophoresis involves the movement of charged particles in a stationary liquid (7,8). The most important electrokinetic mechanisms for the removal of soluble ions from the pore liquid in concrete are electromigration and electroosmosis.

This paper presents a one-dimensional electrokinetics model that evaluates the use of electrokinetics for the removal of ionic species of the radiological contaminants, ^{137}Cs, ^{238}U and ^{90}Sr, from bulk concrete. The model is useful for estimating the power requirements and the rate of contaminant transport during the electrokinetic remediation of concrete.

EQUATION DEVELOPMENT

One of the governing equations for electrokinetic decontamination is the equation of continuity, commonly called the convective diffusion equation. When parallel-plate

electrodes are used, electrokinetic decontamination can be modeled as a one-dimensional problem. The resulting expression for the convective diffusion equation is given below (9):

$$\varepsilon \frac{\partial c_i}{\partial t} = \varepsilon \frac{D_i}{\tau^2} \frac{\partial^2 c_i}{\partial x^2} - \frac{\varepsilon}{\tau^2} \frac{\partial [c_i (u_{e,i} + u_c)]}{\partial x} - (1 - \varepsilon) \rho_b \frac{\partial q_i}{\partial t} + R_i \qquad (1)$$

where,

ε	=	porosity of concrete,
c_i	=	concentration of component *i* in the concrete pore,
t	=	time,
τ	=	tortuosity,
D_i	=	diffusivity of component i,
x	=	distance,
u_c	=	convection velocity, $u_c = (\varepsilon/\mu)\langle\zeta \partial\phi/\partial z\rangle$,
$u_{e,i}$	=	electromigration velocity, $u_{e,i} = v_i z_i F \partial\phi/\partial z$,
v_i	=	mobility of ions, D/RT.
z_i	=	charge number,
F	=	Faraday constant,
q_i	=	solute loading on concrete, grams of solute/grams of concrete,
R_i	=	rate of formation/depletion of solute *i* by chemical and electrochemical reactions.
ϕ	=	potential,
μ	=	viscosity,
ρ_b	=	density of concrete, grams concrete/volume of concrete,
ζ	=	zeta potential.

To simplify matters in the application of the solid-phase material balance, it is often possible to replace the adsorption/desorption kinetics with an overall linear rate expression (10,11). Then the adsorbed-phase mass balance for component *i* is:

$$\rho_b \frac{\partial q_i}{\partial t} = k_{i'} (c_i - c_i^*) \qquad (2)$$

This expression assumes that the mass transfer resistances to the liquid film, surface diffusion, and internal pore diffusion can be lumped into a single rate constant. The overall

mass transfer constant k_i' can be estimated from the physical characteristics of the concrete and the diffusivities of the various solutes. An expression for equilibrium concentration, c_i^*, is required to solve equation 2. Such an expression is obtained by fitting experimental data to various adsorption isotherm models.

The following one-dimensional electrical current density expression is the second equation that governs the electrokinetic decontamination of concrete:

$$i_x = \frac{1}{\tau^2}\left[-\kappa(x)\frac{\partial \phi}{\partial x} - F\sum_{i=1}^{m} z_i D_i \frac{\partial c_i}{\partial x}\right] \tag{3}$$

In the model that will be used to model the electrokinetic decontamination of concrete, it will be assumed that the material conductivity is comprised of two components, surface conductivity and solution conductivity, added in parallel such that $\kappa(x)$ is the effective conductivity of the pore liquid. The conductivity is given by the expression

$$\kappa(x) = F^2 \sum_i z_i^2 v_i c_i + \kappa_{surface} \tag{4}$$

The surface conductivity must be measured experimentally.

In this work, the ions are assumed to be fully disassociated in the liquid phase. The law of electroneutrality applies and is incorporated in the model.

Equations 1, 2, and 3 can be expressed in the following dimensionless forms

$$\frac{\partial \bar{c}_i}{\partial \bar{t}} = \alpha \frac{\partial^2 \bar{c}_i}{\partial \bar{x}^2} + \beta\left[\frac{\partial \bar{c}_i}{\partial \bar{x}}\frac{\partial \bar{\phi}}{\partial \bar{x}} + \bar{c}_i \frac{\partial \bar{\phi}^2}{\partial \bar{x}^2}\right] - Pe\left\langle\frac{\partial \bar{\phi}}{\partial \bar{x}}\right\rangle \frac{\partial \bar{c}_i}{\partial \bar{x}} + \frac{\partial \bar{q}_i}{\partial \bar{t}} + D_i \bar{R}_i \tag{5}$$

$$\bar{i}_x = -\left[\sum_i \Lambda_i^{(1)} \bar{c}_i + \sum_i \Lambda_i^{(2)} \frac{\partial \bar{c}_i}{\partial \bar{x}}\right] \tag{6}$$

$$\frac{d\bar{q}}{dt} = \frac{k' L^2 \rho_p (1-\varepsilon)}{\rho_p D_i \varepsilon}\left(\bar{c} - \bar{c}^*\right) \tag{7}$$

where

$\bar{c}_i$ = dimensionless concentration of component i, c_i/c_{ref},

$\bar{c}_i^*$ = dimensionless equilibrium concentration of component i, c_i^*/c_{ref},

c_{ref} = reference concentration,

$\bar{t}$ = dimensionless time, $t\,D_l/L^2$,

D_l = diffusion coefficient of reference species,

L = thickness of concrete slab,

$\bar{x}$ = dimensionless axial distance, x/L,

$\bar{\phi}$ = scaled electrical potential, ϕ/ϕ_0,

ϕ_0 = reference potential,

$\bar{R}_i$ = scaled reaction rate, R_i/R^0,

R^0 = reference reaction rate,

$\bar{q}_i$ = dimensionless mass loading of component i on concrete, $[\rho_p(1-\varepsilon)]/(c_{ref}\varepsilon)\,q_i$,

$\bar{i}_x$ = dimensionless electrical current density for straight pore, $(RTL)/(F^2D_lc_{ref}\tau^2\phi_0)i_x$,

$\bar{i}_y$ = dimensionless effective electrical current density, $(RTL)/(F^2D_lc_{ref}\tau^2\phi_0)i_x$,

R = universal gas constant,

T = temperature,

α = $D_i/(\tau^2D_l)$,

β = $z_iD_iF\phi_0/(\tau^2D_l)$,

Pe = $\varepsilon_r\varepsilon_0\zeta\phi_0/(\tau^2D_l\mu)$,

ε_r = dielectric constant,

ε_0 = permittivity of free space,

ζ = zeta potential,

μ = viscosity,

Da = $(L^2R^0)/(D_lc_{ref})$,

$\Lambda_i^{(1)}$ = $(z_i^2D_i)/(\tau^2D_l)$,

$\Lambda_i^{(2)}$ = $(z_iD_iRT)/(FD_l\phi\tau^2)$.

Two additional sets of equations are required to model the electrokinetic experiment. Mass balances must be done on the vessels containing the anodes and cathodes. If the vessels are stirred, the dimensionless form of the governing equation is given below:

$$\frac{d\bar{c}_{i,}}{d\bar{t}} = (\pm)\,A_c\left[\beta\frac{d\bar{\Phi}}{d\bar{z}} - Pe\left\langle\frac{\partial\bar{\phi}}{\partial\bar{z}}\right\rangle\right]\bar{c}_i \qquad (8)$$

where

A_c = dimensionless area, $\tau(\varepsilon\pi L d^2)/(4V_{tank})$,
d = diameter of the concrete disk,
$(\pm)$ = +1 for vessel containing the anode and -1 for vessel containing the cathode,
$c_{i,\pm}$ = molar concentration of species i in vessel containing the anode (+) and cathode (-),
V_{tank} = volume of vessel containing the anode or cathode.

Boundary and initial conditions are used that approximate the state of the experimental system. The general initial and boundary conditions are:

in the vessels containing the anode and cathode

$c_{i,+}(0)=c_{i,+}^0$,

$c_{i,-}(0)=c_{i,-}^0$,

in the concrete slab

$c_i(0,x)=c_i^0(x)$ and $q_i(0,x)=q_i^0(x)$,

$c_i(t,0)=c_{i,+}$ when $(u_{e,i}-u_c)>0$,

$c_i(t,x)=c_{i,-}$ when $(u_{e,i}-u_c)<0$.

Subject to the appropriate boundary conditions, equations 5, 6, and 7 are solved by the orthogonal collocation method. Time integrations are performed by the Euler method.

SIMULATIONS

Figure 1 shows a schematic of the electrokinetic computer experiment that was performed to determine the rate of transport of uranyl tricarbonate anion, $UO_2(CO_3)_3^{4-}$, by electromigration. These simulations were also done to evaluate the effect of the number of collocation points in the numerical solution system on (1) the variation of $[UO_2(CO_3)_3^{4-}]$ in the vessels containing the anode and cathode and (2) the axial variation of $[UO_2(CO_3)_3^{4-}]$ in the liquid phase in the concrete.

In these simulations there was no uranium present initially in the anolyte or the catholyte; the only source of uranium was in the concrete pore solution. In addition, all uranium was present in a $UO_2(CO_3)_3^{4-}$ state, with no sorption or precipitation. The initial concentrations of the uranyl tricarbonate and Ca^{2+} in liquid phase were 2.06×10^{-4} M and

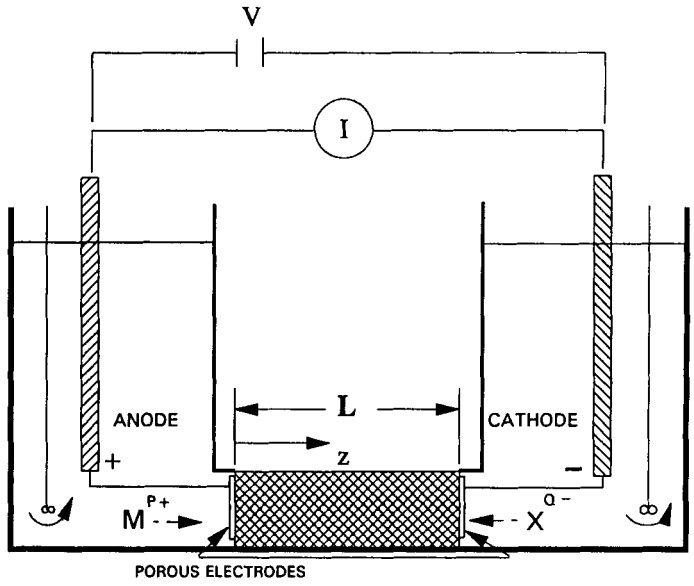

FIGURE 1. Schematic of system used in simulation of dynamic experiments.

0.008 M, respectively. The current density was 5 A/m^2 and the diffusion coefficient for all ions was assumed to be 1.0 x 10^{-9} m/s^2.

The stability of the model and the suitability of the solution method were determined by varying the number of collocation points in the solution system. Figures 2 through 5 show results for simulations using 12, 22 (Figures 3-5 only) and 32 collocation points. Figure 2 shows little effect of the number of collocation points on $[UO_2(CO_3)_3^{4-}]$ in the vessels containing the anode and cathode. Figures 3 through 5 show a greater effect of the number of collocation points on the variation of $[UO_2(CO_3)_3^{4-}]$ along the axial position in the concrete slab. With a few collocation points, the solution oscillates around the solution. The oscillations are suppressed as the number of collocation points are increased. These results suggest that only 12 collocation points are required when only the variation of $[UO_2(CO_3)_3^{4-}]$ is to be computed. However, as many as 32 collocation points are required if the axial variation of $[UO_2(CO_3)_3^{4-}]$ is to be computed accurately.

Figures 6a, 6b, 7a, and 7b present the results of simulations used to illustrate the effect of electroosmosis on the transport of Cs^+ and $UO_2(CO_3)_3^{4-}$ from the liquid phase in the concrete. The conditions for the Cs^+ simulation are similar to those for $UO_2(CO_3)_3^{4-}$; as

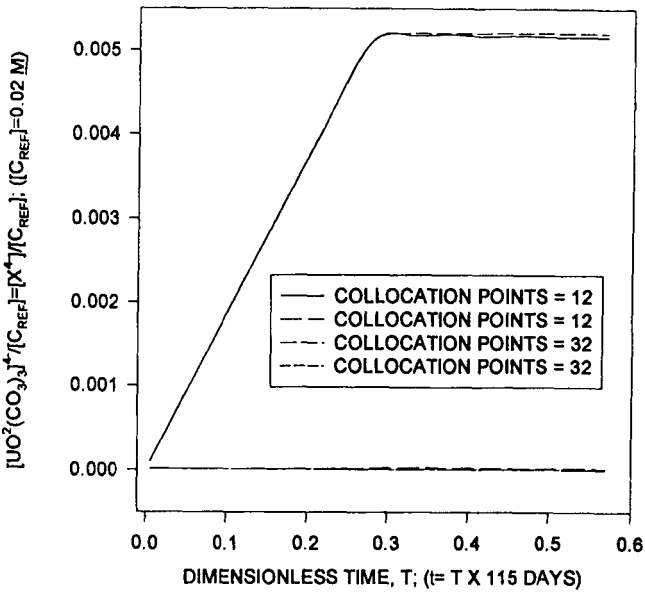

FIGURE 2. Effect of number of collocation points on computed $UO_2(CO_3)_4^{4-}$ concentration in the anolyte (top curves) and catholyte (bottom curves). ($[Ca^{2+}]_{+,c_i}$=0.008 M, i=5mA/m^2, $[UO_2(CO_3)_4^{4-}]$=2.06x10^{-4} M, D_i=1x10^{-9}m^2/s, L=10 cm, V_1=V_2=100 cm^3, t=10)

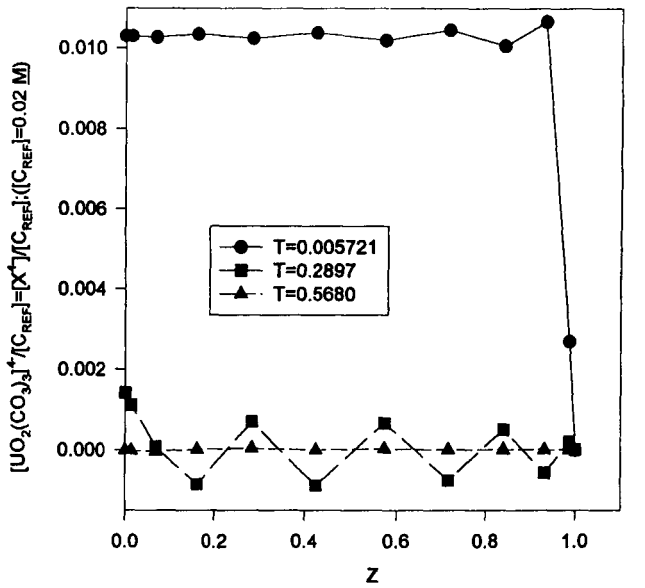

FIGURE 3. Computed $UO_2(CO_3)_4^{4-}$ concentration profile in concrete for 12 collocation points. ($[Ca^{2+}]_{+,c_i}$=0.008 M, $[UO_2(CO_3)_4^{4-}]$=2.06x10^{-4} M, D_i=1x10^{-9} m^2/s, i=5 mA/m^2, L=10 cm, V_1=V_2=100 cm^3, t=10)

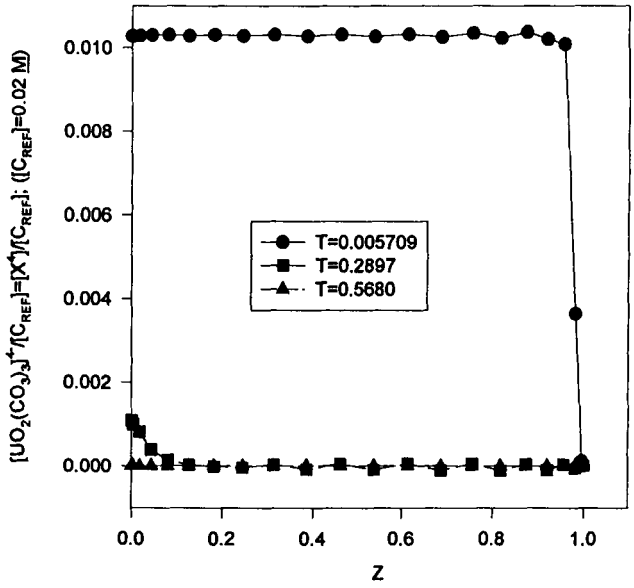

FIGURE 4. Computed $UO_2(CO_3)_4^{4-}$ concentration profile in concrete for 22 collocation points. ($[Ca^{2+}]_{+c_i}$=0.008 M, $[UO_2(CO_3)_4^{4-}]$=2.06x10^{-4} M, D_i=1x10^{-9} m^2/s, i=5 mA/m^2, L=10 cm, $V_1=V_2$=100 cm^3, t=10)

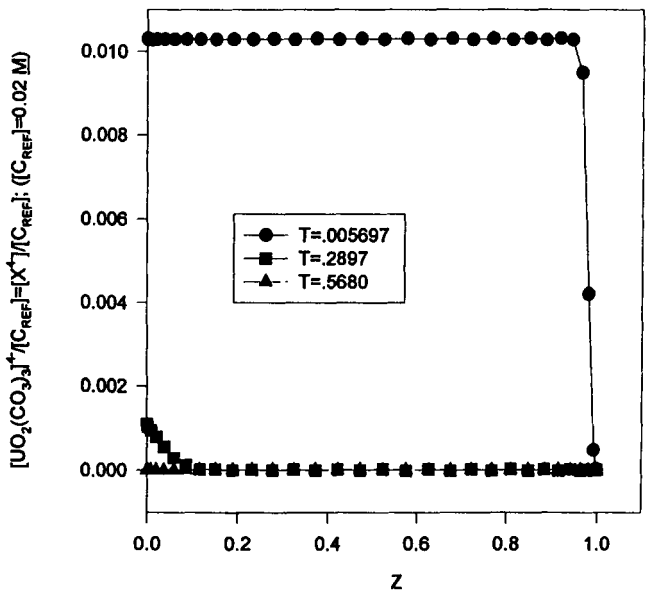

FIGURE 5. Computed $UO_2(CO_3)_4^{4-}$ concentration profile in concrete for 32 collocation points. ($[Ca^{2+}]_{+c_i}$=0.008 M, $[UO_2(CO_3)_4^{4-}]$=2.06x10^{-4} M, D_i=1x10^{-9} m^2/s, i=5 mA/m^2, L=10 cm, $V_1=V_2$=100 cm^3, t=10)

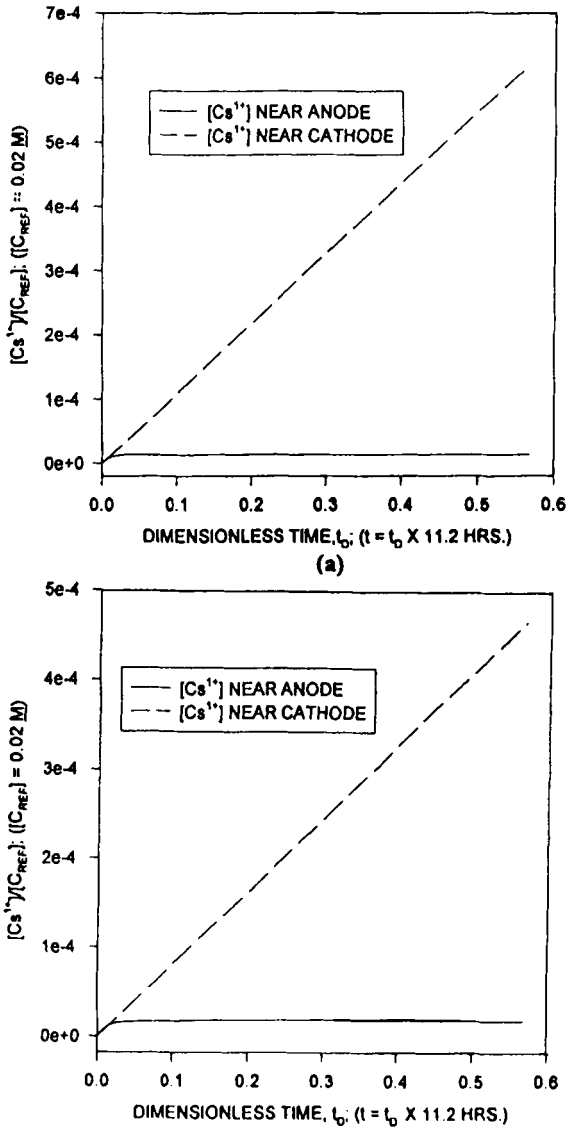

FIGURE 6. Computed electrokinetic transport of Cs^{1+} through a concrete core: (a) without electroosmosis; (b) with electroosmosis. ($[Ca^{2+}]_{+c.}$=0.008 M, $[UO_2(CO_3)_4^{4-}]$=2.06x10^{-4} M, $[Cs^{1+}]$=4.52x10^{-4} M, D_i=1x10^{-9} m^2/s, i=5 mA/m^2, L=10 cm, V_1=V_2=100 cm^3, t=10)

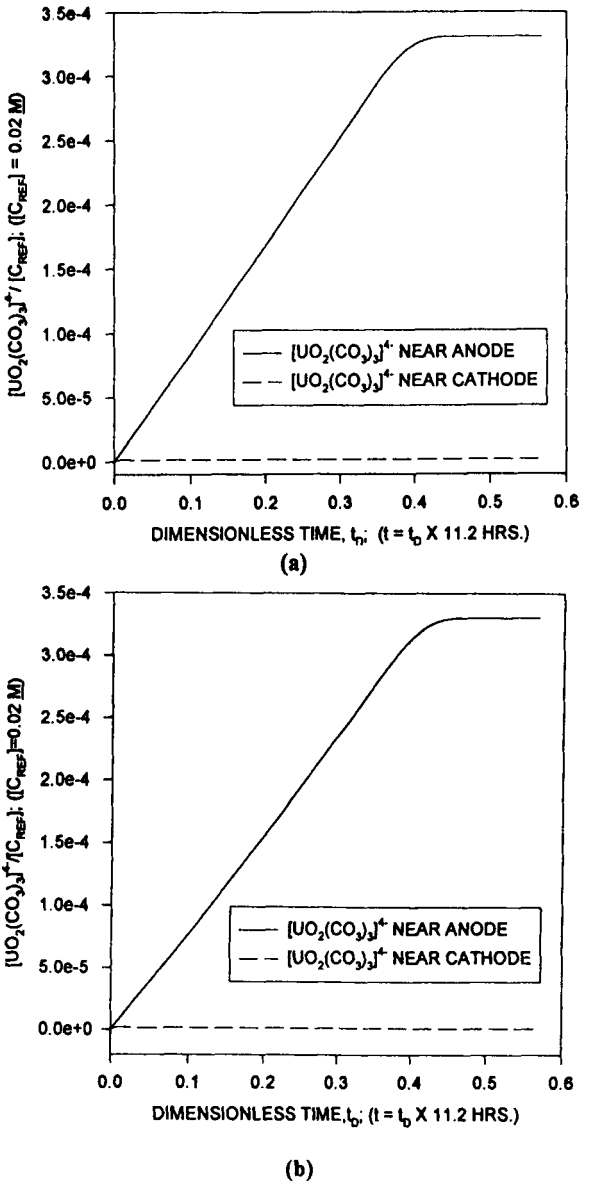

FIGURE 7. Computed electrokinetic transport of $UO_2(CO_3)_4^{4-}$ through a concrete core: (a) without electroosmosis; (b) with electroosmosis. ($[Ca^{2+}]_{t.c.}$=0.008 M, $[UO_2(CO_3)_4^{4-}]$=2.06x10^{-4} M, $[Cs^{1+}]$=4.52x10^{-4} M, D_i=1x10^{-9} m^2/s, i=5 mA/m^2, L=10 cm, V_1=V_2=100 cm^3, t=10)

with the previous simulations, the concrete pore liquid is the only source of the contaminants, and there are no sorption or precipitation effects. The thickness of the concrete slab, L, was 0.635 cm, and the initial concentration of Ca^{2+} was 0.008 M. The current density was 47.8 A/m^2 for these simulations, and a zeta potential of -20 mV was used in the computations that included electromigration. As reported by DePaoli et al.(12), the zeta potential varied from -40 mV to 4 mV and depends on the presence of potential-determining ions such as sodium and calcium. The -20-mV value thus represents an average zeta potential. Comparing Figures 6a, 6b, 7a, and 7b, it is seen that although electrosmosis enhances the transport of Cs^+ to the cathode and retards the migration of uranyl tricarbonate to the anode, electromigration is the dominant transport mechanism. These figures also show the effect of the charge number, z_i, on the electromigration of Cs^+ and $UO_2(CO_3)_3^{4-}$. The uranyl tricarbonate is transported to the anode much faster than the Cs^+ migrates to the cathode. The $[UO_2(CO_3)_3^{4-}]$ in the anolyte reaches steady state in approximately 0.4 dimensionless time units, whereas the $[Cs^+]$ did not reach a steady-state value after 0.6 dimensionless time units (12).

COMPARISON OF COMPUTATIONAL AND DYNAMIC EXPERIMENTAL RESULTS

Computer runs were conducted to simulate the conditions of the dynamic experiments that were conducted with cesium and strontium. These simulations included sorption/ion exchange effects on the concrete by incorporating the isotherms that were measured in the equilibration tests (13).

CESIUM

As described by DePaoli et al. (12), bench-scale experiments were performed where the initial anolyte solution was 0.016 M sodium hydroxide with 0.00752 M cesium and the catholyte was 0.016 M sodium hydroxide. The concrete slab was 3.81 cm in diameter and 0.952 cm thick. The current was 0.1 A,and the potential drop across the anode and cathode varied from approximately 50 to 100 V. If it is assumed that the current flux is across the entire cross-sectional area of the concrete, the current density, i_z, was 87.7A/m^2. Since the porosity of concrete is approximately 0.2 to 0.4 (14), the current density in the pores would be approximately 438 to 219 A/m^2. Table 1 shows a listing of the ions included in the simulations and their assumed initial concentrations in the anolyte, catholyte, and concrete pore solution, and Table 2 lists the parameter values that were used.

The comparison between the experimental and simulation results is shown in Figures 8 through 10. The concentration of cesium and sodium hydroxide is 0.00752 *M* in the

Table 1. INITIAL CONCENTRATIONS OF IONS FOR SIMULATION OF CESIUM DYNAMIC EXPERIMENT.

Ion	Anolyte (M)	Pore Solution (M)	Catholyte (M)
Ca^{2+}	0	0.005	0
Na^{+}	0.016	0	0.016
H_3O^{+}	$6.3x10^{-13}$	$1.0x10^{-12}$	$6.3x10^{-13}$
OH^{-}	0.016	0.010	0.016
NO_3^{-}	0.0075	0	0
Cs^{+}	0.0075	0	0

vessel containing the anode and 0.016 *M* throughout the system, respectively. The cesium cations are transported by electromigration from the anolyte, through the concrete slab to the catholyte. Sorption is allowed to occur in the concrete slab according to experimentally measured isotherms. A current density of 219A/m^2 was used in the computer simulations. Figure 8 shows the transport of Cs^{1+} from the anolyte, through the concrete and to the catholyte. The computer model accurately predicts the rate of transport of Cs^{1+} from the anolyte and into the concrete. However, the computer code overpredicts the rate of transport of Cs^{1+} to the catholyte. The dimensionless mass transfer coefficient for the transport of Cs^{1+} from the liquid to the solid phase is 40.

Figure 9 shows the computed and experimental variation of the pH during the electrokinetic decontamination of concrete. The computer model captures the trend in the variation of the pH; however, the quantitative agreement between the computed and experimental results is fair. The discrepancy between the two results is possibly due to the assumption in the model that the $[Ca^{2+}]$ in the pore liquid is constant over the entire simulation. Future improved versions of this model should include the desorption/dissolution of Ca^{2+} from pore walls in the concrete.

The variation of the voltage drop, ΔV, across the concrete core is illustrated in Figure 10. Like the pH results, the computer model predicts the trend in ΔV; however, there is

Table 2. PARAMETER VALUES FOR SIMULATION OF CESIUM DYNAMIC EXPERIMENT

Parameter	Value
Da	0
Pe	0
α_i	0.030
β_{Ca}	2.322
β_{Na}, β_H, β_{Cs}	1.161
β_{OH}, β_{NO3}	-1.161
$\Lambda^{(1)}_{Ca}$	0.120
$\Lambda^{(2)}_{Ca}$	0.00155
$\Lambda^{(1)}_{Na}$, $\Lambda^{(1)}_{Cs}$	0.030
$\Lambda^{(2)}_{Na}$, $\Lambda^{(2)}_{Cs}$	7.77×10^{-4}
$\Lambda^{(1)}_{NO3}$, $\Lambda^{(1)}_{OH}$	0.030
$\Lambda^{(2)}_{NO3}$, $\Lambda^{(2)}_{OH}$	-7.77×10^{-4}
τ	-7.77×10^{-4}

only semiquantitative agreement between the data. Similar to the pH, ΔV depends on the concentration of ions in pores of the concrete. Thus, it is expected that the agreement between the experimental and computed results would improve if better models were used for the sorption/dissolution/ion exchange of ions in the pores of the concrete.

Strontium

As described by DePaoli et al. (12), a bench-scale experiment was performed in which the initial anolyte solution was 0.016 M sodium hydroxide with 0.0114 M strontium

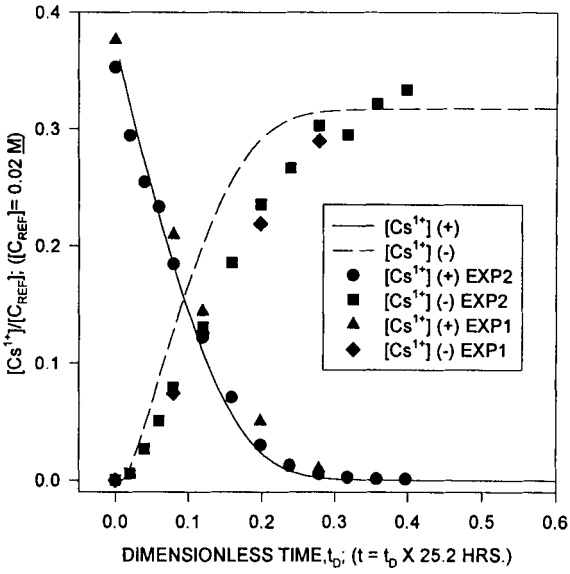

FIGURE 8. Comparison of computed and experimental cesium concentration in anolyte and catholyte. (D_i=1x10^{-9} m^2/s, i=0.834, e=0.4, L=0.952 cm, V_1=V_2=200 mL, t=5.77, A_c=0.1252, k'=10, q'(0,z)=0)

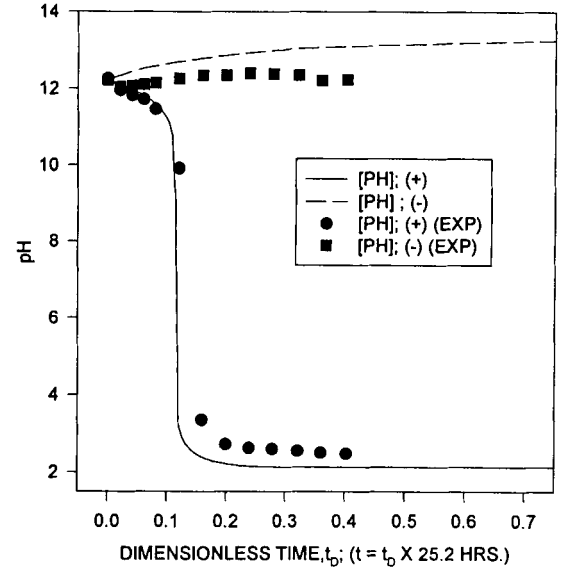

FIGURE 9. Comparison of computed and experimental pH during cesium transport.

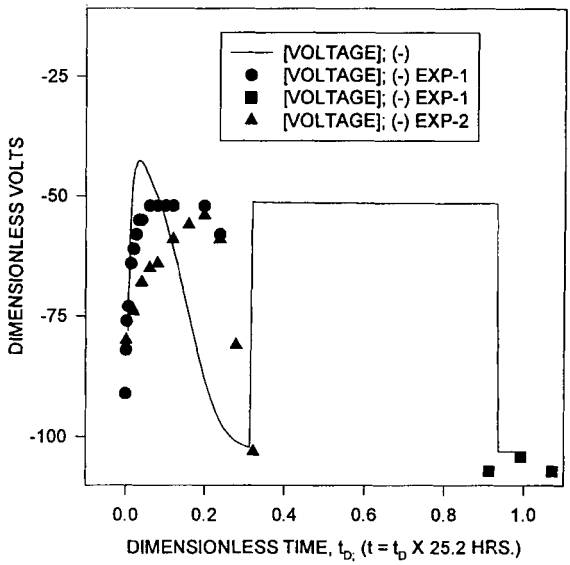

FIGURE 10. Comparison of computed and experimental voltage drop across concrete disk during cesium transport.

nitrate and the catholyte was 0.016 M sodium hydroxide. The experimental setup and operating conditions (i=100 mA) were similar to those that were used in the cesium dynamic experiments.

Strontium will exist as either $Sr(OH)^+$ or precipitate as a carbonate in the very alkaline (pH>13) (15) pore liquid in the concrete. Thus, the simulations were performed as if strontium existed in the monovalent hydroxide state. The major ions in the pore liquid are assumed to be same as those given in Table 1 except for the replacement of $Sr(OH)^+$ for Cs^+. Since the size of the strontium monohydroxide is approximately twice that of the cesium cation, the diffusivity (5×10^{-9} m^2/s) for the strontium monohydroxide ion is approximately half that of cesium. The initial concentrations of the ions and parameter values for the simulation the electrokinetic transport of strontium through concrete are given in Tables 3 and 4, respectively. The simulation results are presented in Figures 11 to 13. Figure 11 shows the comparison of the simulated and experimental results for the variation of the strontium concentration in the anolyte and catholyte. There is good agreement between the simulated and experimental results.

Table 3. INITIAL CONCENTRATIONS OF IONS FOR SIMULATION OF STRONTIUM DYNAMIC EXPERIMENT

Ion	Anolyte (M)	Pore Solution (M)	Catholyte (M)
Ca^{2+}	0	0.008	0
Na^{+}	0.016	0	0.016
H_3O^{+}	$6.3x10^{-13}$	$6.3x10^{-13}$	$6.3x10^{-13}$
OH^{-}	0.016	0.016	0.016
NO_3^{-}	0.0228	0	0
Sr^{2+}	0.0114	0	0

The simulated and experimental pH and voltage data are presented in Figures 12 and 13, respectively. These figures illustrate that, similar to the cesium data, the computer model captures the trend in the experimental pH and voltage data. Again, better models are required to account for the fate of ions in the pores of the concrete.

DISCUSSION OF RESULTS

A one-dimensional model has been developed for the electrokinetic decontamination of concrete. The model shows that electromigration is the dominant transport mechanism for the removal of cations and anions such as Cs^{+} and $UO_2(CO_3)_3^{4-}$. Electromigration is strongly affected by the charge number of ions. Furthermore, the results from the simulations suggest that even if ions are sorbed onto the solid cement particles or pore walls, electrokinetics can still be used to decontaminate concrete if the proper lixiviant is employed to produce a favorable sorption isotherm. The model was tested by comparing its results with bench-scale experimental data for Cs and for Sr. There was good agreement between the model and the batch experiments.

Additional modifications are required for more accurate prediction of contaminant transport using EK. One recommended revision to this one-dimensional model is a mechanism for the desorption of Ca^{2+} from the solid phase. Further valuable revisions

Table 4. PARAMETER VALUES FOR SIMULATION OF STRONTIUM DYNAMIC EXPERIMENT

Parameter	Value
Da	0
Pe	0
$\alpha_{Sr(OH)}$	0.015
α_i ($i = Ca^{2+}, Na^+, NO_3^-$)	0.030
β_{Ca}	2.322
β_{Na}, β_{H3O}	1.161
$\beta_{Sr(OH)}$	0.581
β_{OH}, β_{NO3}	-1.161
$\Lambda^{(1)}_{Ca}$	0.120
$\Lambda^{(2)}_{Ca}$	0.00155
$\Lambda^{(1)}_{Na}$	0.030
$\Lambda^{(2)}_{Na}$	7.77×10^{-4}
$\Lambda^{(1)}_{Sr(OH)}$	0.015
$\Lambda^{(2)}_{Sr(OH)}$	3.89×10^{-4}
$\Lambda^{(1)}_{NO3}$, $\Lambda^{(1)}_{OH}$	0.030
$\Lambda^{(2)}_{NO3}$, $\Lambda^{(2)}_{OH}$	-7.77×10^{-4}
τ	5.77

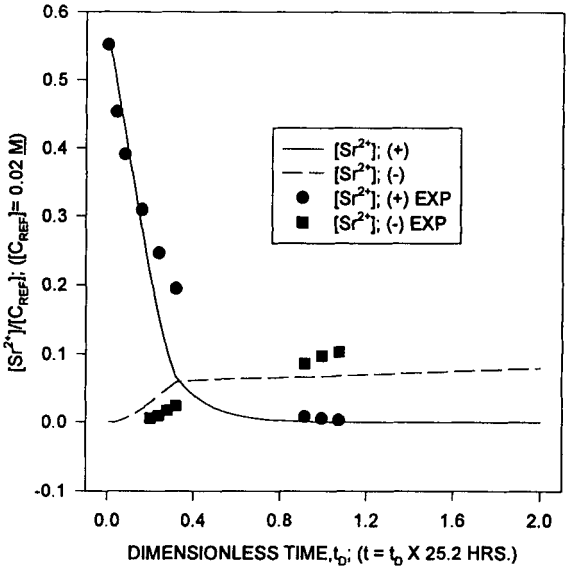

FIGURE 11. Comparison of computed and experimental strontium concentration in anolyte and catholyte. (D_i=1x10^{-9} m^2/s, i=0.834, e=0.4, L=0.952 cm, V_1=V_2=200 mL, t=5.77, A_c=0.1252, k'=10, q'(0,z)=0)

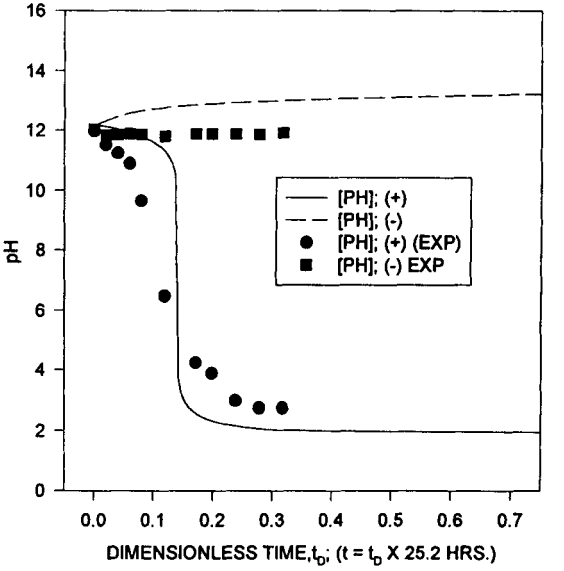

FIGURE 12. Comparison of computed and experimental pH during strontium transport.

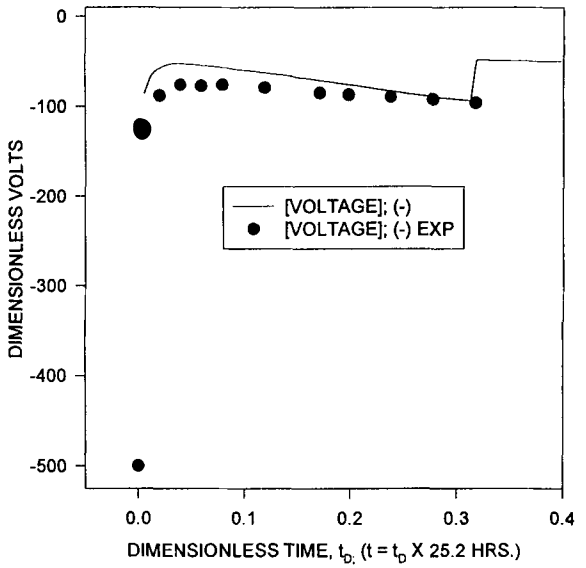

FIGURE 13. Comparison of computed and experimental voltage drop across concrete disk during strontium transport.

would include expansion to a two-dimensional domain, which would allow modeling of dual-reservoir EK systems.

CONCLUSIONS

The results of a one-dimensional computational model have been shown to be in good agreement with dynamic experiments; therefore, this model will provide a valuable tool for the further investigation and optimization of the application of electrokinetic decontamination of concrete. The experimental and theoretical work that has been conducted has served to answer several questions regarding the technical feasibility of the process; however, the ultimate utility of the process must be determined through demonstration. The operating conditions for a demonstration should be optimized by simulation using a model such as that developed in this work. This model would allow estimation of the amount of contaminant removed and the time required for cleanup for a given applied voltage/current.

Further development of the electrokinetics model is required for dual-reservoir process designs. A two-dimensional model is necessary to determine the capabilities and limitations of dual-reservoir process designs. Two-dimensional modeling would result in a mapping of the spatial distribution of electrical current under different geometries. This would aid in system design by helping to avoid short-circuit current flow along the surface between electrolyte reservoirs and to ensure that current flow is significantly deep to encompass the entire contamination zone.

ACKNOWLEDGEMENT

The authors wish to thank N. Cate and K. Heath for their assistance. This research was sponsored by the U.S. Department of Energy (DOE) Office of Technology Development within the Office of Environmental Restoration and Waste Management (EM).

REFERENCES

1. Murphie, W. E., "Decommissioning of Radioactive Facilities," Proc. Intl. Conf. Institution of Mechanical Engineers, Feb. 17-19, London, United Kingdom, 1992, p. 9.

2. Dickerson, K. S., Wilson-Nichols, M. J., and Morris, M. I., Contaminated Concrete: Occurrence and Emerging Technologies for DOE Decontamination, DOE/ORO-2034, 1995.

3. Harris, M. T., and Basaran, O. A. "Capillary Electrohydrostatics of Conducting Drops Hanging from a Nozzle in an Electric Field," J. Colloid Interface Sci. 161, 389 (1993).

4. Bostick, W. D., et al., Electroosmotic Decontamination of Concrete, Martin Marietta Energy Systems, Inc., Oak Ridge, Tennessee, K/TCD-1054, 1993.

5. Morgan, I. L., and Gilbert, V. P., Testing of Non-Destructive Concrete Decontamination Techniques for the Solar Basins at the Hanford Site (draft), Oak Ridge National Laboratory, Oak Ridge, Tennessee, 1994.

6. Atkins, P. W., Physical Chemistry, W. H. Freeman, San Francisco, California, 1982.

7. Adamson, A. W., Physical Chemistry of Surfaces, John Wiley and Sons, Inc., New York (1990).

8. Evans, D. F., and Wennerstrom, H., The Colloidal Domain: Where Physics, Chemistry, Biology and Technology Meet, VCH Publishers, Inc., New York, New York (1994).

9. Shapiro, A. P., Electoosmotic Purging of Contaminants from Saturated Soils, PhD thesis, Massachusetts Institute of Technology (1990).

10. Santacesaria, E.M., et al., "Separation of Xylenes on Y Zeolites 2. Breakthrough Curves and Their Interpretation," Ind. Eng. Chem. Process Des. Dev., 21, 446 (1982).

11. Carta, G., FXCOLFRF.F77: A FORTRAN 77 Computer program, University of Virginia, 1986.

12. DePaoli, D.W., et al., Testing and Evaluation of Electrokinetic Decontamination of Concrete, DOE/ORO/2036, 1995.

13. DePaoli, D.W., Harris, M.T., Morgan, I. L., and Ally, M.R., "Investigation of Electrokinetic Decontamination of Concrete," submitted to Sep. Sci. Technol. (1995).

14. Taylor, H.F.W., Cement Chemistry, Academic Press Inc., Orlando, Florida (1990).

15. Baes, C.F., Jr. and Mesmer, R.E., The Hydrolysis of Cations, John Wiley and Sons, New York (1976).